Mitigating loads by means of an active slat

IOP Conf. Series: Journal of Physics: Conf. Series **1037** (2018) 022032 doi:10.1088/1742-6596/1037/2/022032

Mitigating loads by means of an active slat

L Neuhaus[1], P Singh[1], T Homeyer[1], O Huxdorf[2], J Riemenschneider[2], J Wild[3], J Peinke[1] and M Hölling[1]

[1]ForWind - Institute of Physics, University of Oldenburg, 26129 Oldenburg, Germany
[2]DLR - Institute of Composite Structures and Adaptive Systems, 38108 Braunschweig, Germany
[3]DLR - Institute of Aerodynamics and Flow Technology, 38108 Braunschweig, Germany

E-mail: lars.neuhaus@uni-oldenburg.de, piyush.singh@uni-oldenburg.de

Abstract. An active slat on an airfoil is tested in the wind tunnel to reduce lift fluctuations caused by inflow angle fluctuations. The airfoil with an integrated slat allows to control the gap size between slat and main body. The variation of the gap size leads to different aerodynamic properties. This behavior is investigated in a comprehensive characterization of the aerodynamics for different positions of the static slat and a wide range of angles of attack. A sinusoidal inflow angle fluctuation is generated by an active grid. These fluctuations are causing lift force fluctuations at the airfoil with static slat. The slat gap size then is varied dynamically synchronous to the inflow angle fluctuations. Depending on the phase shift between slat gap size variation and inflow angle fluctuation a reduction of the lift force is observed. The slat system is found to be capable of mitigating load fluctuations caused by turbulent inflow.

1. Introduction

Wind turbines are exposed to turbulent wind conditions mainly due to their presence in the atmospheric boundary layer [1]. High and fast velocity changes can be observed under such circumstances. Depending on the radial position on the blade, these wind velocity fluctuations lead to fluctuations of the local inflow angle of several degrees. For the aerodynamic profiles of the blades these fluctuations lead to local fluctuations of the lift and drag forces, which in turn cause load variations on the wind turbine blades. Larger fluctuating forces are responsible for higher damage equivalent loads and may reduce the overall lifetime and efficiency of the wind turbine blade [1]. This locally varying inflow can not be handled by a common pitch control system of the whole blade.

In order to reduce the effect of local inflow angle fluctuations the concept of a deformable active slat system is investigated. A slat system exhibits the benefit of an enlarged operating angle of attack range and stall delay [2]. With the active slat different aerodynamic coefficients for the same inflow angle can be achieved by a variation of the slat gap size [3]. For varying inflow angles, the slat can be moved to different positions to reduce the resulting load changes. As the slat system has much less mass than a whole blade, the slat concept allows for a fast reaction on local inflow angle fluctuations.

An extensive parametric study is undertaken in order to get a detailed characterization of the slat behavior. The behavior of a 2D airfoil with active slat is studied for different static slat positions for constant inflow angle and for fluctuating inflow angles. The potential of using an

active slat for load reduction is demonstrated via synchronized slat deformations and sinusoidal inflow angle variations.

2. Experimental Setup

The measurements are performed in the Göttingen type wind tunnel at the University of Oldenburg. The test section has a dimension of 1 m × 0.8 m × 2.6 m (width, height, and length respectively). The wind tunnel can generate wind speeds up to $50\,\mathrm{m\,s^{-1}}$ and the turbulence intensity for laminar inflow has been reported to be around 0.3% [4]. An active grid is used for generation of fluctuations of the angle of attack. The active grid consists of 9 independently controllable shafts arranged parallel to the airfoil span, each having a rectangular profile to ensure span-wise correlation of the wind field (figure 1(a)). The inflow angle of the generated turbulent wind field is measured via X-hot-wire anemometry at a sampling frequency of 10 kHz.

An airfoil with an integrated active slat is used in this measurement campaign. The aerodynamic non-deformed profile for the shape-adaptive slat is optimized based on the DU 91-W2-250-profile [5]. The airfoil model chord is 300 mm. At maximum wind speed a Reynolds number related to the airfoil chord of $\mathrm{Re} = 10^6$ is achieved. To prevent an artificial separation by laminar separation bubble burst, the airfoil slat was decently tripped triggering premature laminar-turbulent flow transition. The structural design allows a dynamic variation of the trailing edge position of the slat [6]. The slat can be deformed independently by a stepper motor which enables to change the gap size, g_s, between slat and main body dynamically from $g_s/c = 1.06\%$ up to $g_s/c = 2.83\%$ (3.18-8.49 mm)(figure 2(a)). The aerodynamic reference gap size of the slat is defined to be $g_{s,ref}/c = 2.05\%$.

The airfoil is attached to turn tables in the wind tunnel top and bottom walls on either side of its span (figure 1(b)). The forces acting on the airfoil are measured using a load cell for forces

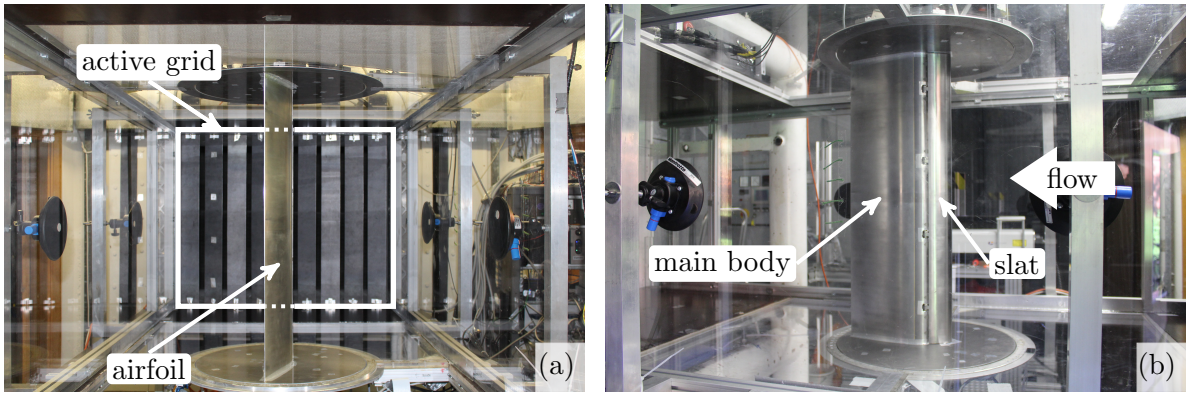

Figure 1: Active grid and airfoil with integrated active slat installed in the wind tunnel (a) and side view of the profile (b).

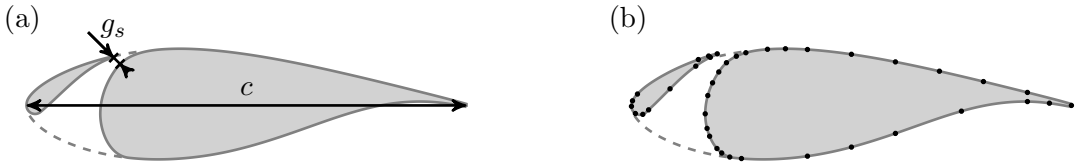

Figure 2: Investigated airfoil with controllable gap size g_s between slat and main body of the airfoil (a) and locations of pressure taps on the airfoil (b).

and a torque sensor placed along the airfoil's mounting axis. Forces and moments are recorded at a sampling frequency of 1 kHz. The rotation axis of the turn tables is at the quarter chord location of the airfoil. The upper turn table is equipped with a stepper motor for pitching the airfoil. A directional sensor is attached to the lower turn table to monitor the pitch angle. The reference wind speed is measured through a Setra C 239 differential pressure transducer and the temperature as well as humidity are measured with a Galltec-Mela DKK200F10SF0500G sensor.

The surface pressure distribution of the airfoil is measured through a total of 40 pressure taps in the integrated slat airfoil at the central span-wise location, with 28 of them positioned on the main body and 12 positioned on the slat. A schematic sketch of the chord-wise cross section representing the distribution of the pressure taps on the airfoil is presented in figure 2(b). The pressure taps are connected to three multi-channel synchronized pressure scanners by tubes passing through the lower turn table. The pressure measurements are done at a sampling frequency of 100 Hz.

3. Results

3.1. Characterization

To assess the influence of the slat on the aerodynamic behavior of the airfoil a parametric study is performed with the varied parameters being the wind speed, the pitch angle of the airfoil, the slat gap size, and fluctuations of the inflow angle. Herein, some results for a wind speed of $30\,\mathrm{m\,s^{-1}}$ with laminar inflow are presented. The aerodynamic behavior of the slotted airfoil is investigated for ten different static gap sizes for a wide range of angles of attack. The airfoil is investigated for angles of attack α from $-20°$ up to $34°$ in $0.5°$ steps for the aerodynamic reference gap size, $g_{s,ref}$. For the other gap sizes, the step size is $1°$ up to $\alpha = 20°$ and $0.5°$ for $\alpha = 20°$ - $34°$. These 730 cases are measured with laminar inflow for which the active grid was removed.

The determined static lift coefficients for the gap variation are shown in figure 3. It can be recognized, that different lift coefficients can be achieved at an angle of attack for different

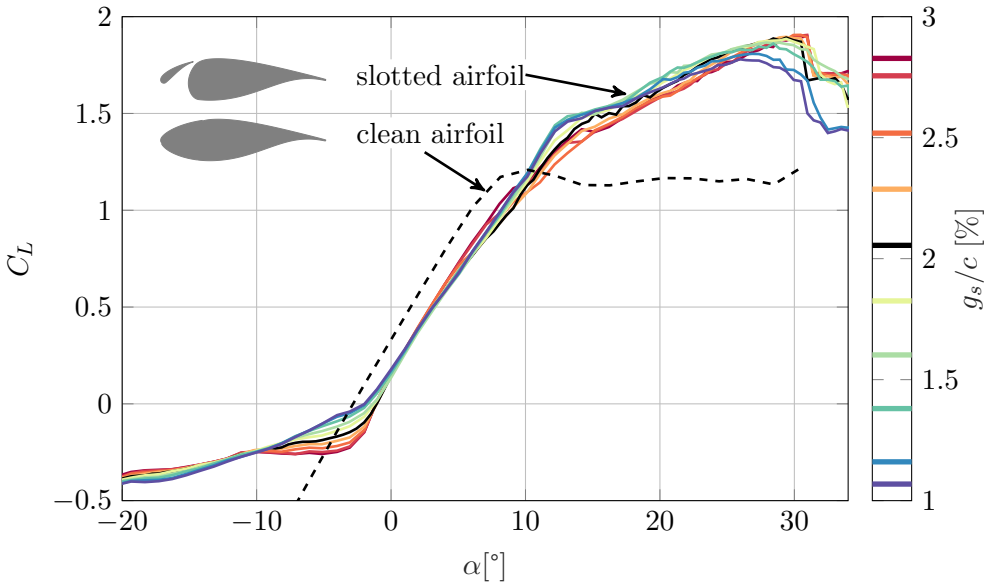

Figure 3: Static lift coefficients C_L for laminar inflow with $\mathrm{Re} = 0.6 \cdot 10^6$ for different gap sizes g_s compared to the clean airfoil without slat.

gap sizes. Compared to the clean airfoil without slat [7], the linear region ($\alpha = -4$ - $9°$) of the lift curve is shifted to higher angles of attacks ($\alpha = -2$ - $13°$). The slotted airfoil achieves an approximately 1.5 times higher maximum lift coefficient at a significantly higher angle of attack. Also the occurrence of stall is shifted to higher angles of attack by the integrated slat as expected. Separation occurs at approximately $\alpha = 10°$ on the clean airfoil, whereas for the integrated slat stall is shifted to approximately $\alpha = 30°$. The slat enables a 2-3 times larger operational angle of attack range compared to the clean airfoil.

To further determine the achievable lift coefficients for the slotted airfoil at a given angle of attack, the difference between the lift coefficient of the airfoil with different gap sizes and the one with the aerodynamic reference gap size, $g_{s,ref}$, is determined for every angle of attack (figure 4). For different angle of attack regions, different dependencies of the lift coefficient on the gap size can be recognized. The airfoil with a bigger gap size produces higher lift coefficients for angles of attack from $\alpha = 1°$ up to approximately $\alpha = 9°$, whereas higher lift coefficients are generated by the smaller gap sizes between $\alpha = 10°$ and $\alpha = 24°$. Furthermore, not necessarily the extreme gap sizes are producing the extreme lift coefficients.

This is found to be connected to the different contributions to lift generation by slat and main body (figure 5). In accordance to the theory of slotted airfoils [2] a more closed gap reduces the suction pressure peak on the main airfoil and increases the circulation of the slat, seen in a stronger suction pressure at the slat upper surface (figure 5 (a,c)). According to the pressure difference the lift coefficient contributions generated by the main body and the slat are behaving as shown in figure 5 (b,d). With increased gap size, g_s, the lift coefficient generated by the main body increases and the one by the slat decreases. The slope of the lift coefficient in function of the gap sizes is always positive for the main body and negative for the slat. This tendency is consistent for different angles of attack, α, although the slopes change depending on the angle of attack. Depending on the magnitudes of the slopes of slat and main body the lift coefficient generated by the whole airfoil shows different non-linear behaviour depending on the gap size for different angle of attacks (figure 5 (b,d)). For $\alpha = 5°$, the lift generated by the whole airfoil is almost linearly increasing with the gap size (figure 5(b)). Whereas, for $\alpha = 10°$ a different

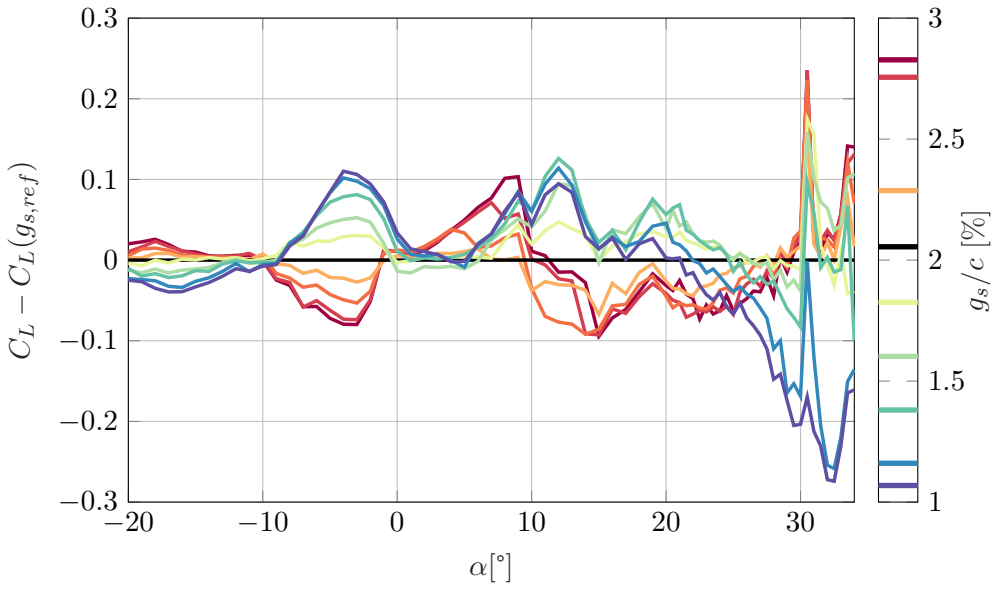

Figure 4: Deviation of the lift coefficient $C_L(g_s)$ for different gap sizes from the lift coefficient $C_L(g_{s,ref})$ for the aerodynamic reference gap size in function of the angle of attack α.

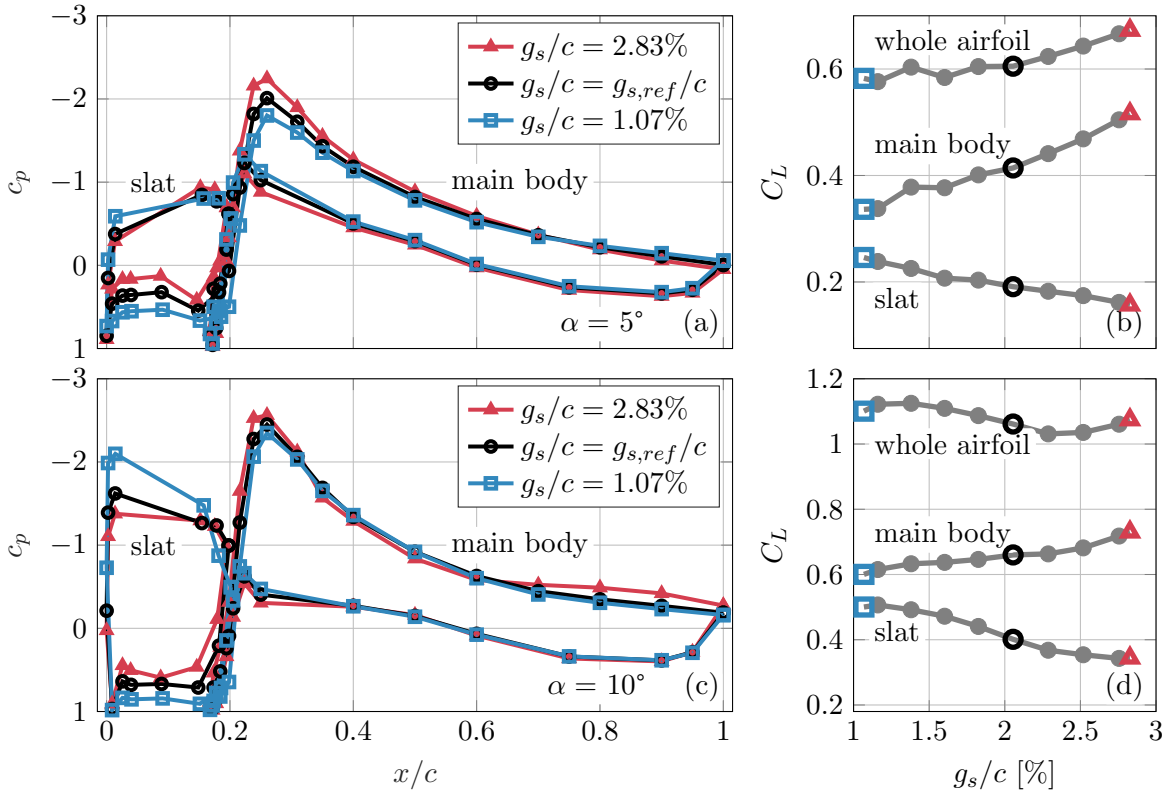

Figure 5: Distribution of the pressure coefficient c_p for different gap sizes g_s (a,c) and the corresponding lift coefficient C_L in function of the gap sizes divided into contributions of C_L produced by slat, main body, and whole airfoil (b,d) for an angle of attack of $\alpha = 5°$ (a,b) and for an angle of attack of $\alpha = 10°$ (c,d).

behavior can be recognized (figure 5(d)). The lift generated by the whole airfoil for $\alpha = 10°$ is first decreasing and then shows an increasing trend with increasing gap size. In this case, the dependency of the lift coefficient with gap size can not be described by a linear function.

It is found, that different gap sizes are producing different lift coefficients for the same inflow angle. However, the lift coefficient is not a simple linear function of the gap size and depends on the angle of attack. A consistent function of the lift coefficient on the gap size for all angles of attack would be beneficial for a control strategy. Despite the non-linearity and angle of attack dependency, as an initial step it is neglected herein to come up with a first trivial control method of the lift.

3.2. Timed Inflow-angle-coupled Motion control (TIM control)

The TIM control refers to a synchronized variation of slat gap size with the motion of the active grid. Although a trivial control strategy, the TIM control may provide the means to assess the initial capabilities of the slat for blade load mitigation. To complement the control strategy, a rather simplistic turbulent inflow condition in the form of a sinusoidal variation of the angle of attack is adopted. The active grid is used to generate fluctuations in the angle of attack without the need of pitching the airfoil and hence without additional inertia forces. First, X-hot-wire measurements are undertaken in the empty closed test section in the center-line at the quarter-chord position of the later installed airfoil. The velocity and the angle of the wind inflow depends mainly on the amplitude and motion speed of the active grid blades. In the presented

case the inflow angle fluctuations are generated by sinusoidal motion of the flaps of the active grid at a frequency of 5 Hz. The inflow angle fluctuations follow this sinusoidal motion with an amplitude of approximately 3° and additional noisy disturbances caused by the wakes and separation on the flaps of the active grid (figure 6(a)).

The same active grid motions are repeated with the airfoil installed at a pitch angle of 10°. For the reference measurements the airfoil slat is kept static at its aerodynamic reference gap size. The created inflow angle fluctuations result in fluctuations of the lift coefficient of about ±0.2 (figure 6(b)). The inflow angle as well as the lift fluctuation time series have a temporal length of 30 s but for legibility only 2 s of data is shown in figure 6 (a) and (b).

As discussed in section 3.1, the lift coefficient can be varied by altering the gap size g_s. This is utilized by the TIM control to lower the lift fluctuation by a sinusoidal variation of the slat trailing edge position and hence an approximately sinusoidal variation of the gap size. The measurements are repeated for 10 different phase shifts, ψ, between slat gap size variations and inflow angle fluctuations. The visual inspection of the C_L time series of the static slat at aerodynamic reference gap size in comparison with the TIM controlled slat with phase shift $\psi = 36°$ shows a reduction in the C_L fluctuations, on the other hand for $\psi = 216°$ the C_L fluctuations are increased (figure 7(a)). The standard deviation of the lift for TIM controlled slat with different ψ is compared with the static slat reference case (figure 7(b)). A reduction of the standard deviation of approximately 20.1 % can be achieved for a phase shift of $\psi = 36°$. For $\psi = 161°$ to $\psi = 324°$ an amplification of the standard deviation of up to 8.4 % by the dynamic slat gap size variation is recognized. However, no significant influence of the phase shift on the drag coefficient is found. Based on the phase shift the standard deviation of the lift coefficient can be reduced by a coupled actuation of active slat and active grid. This control strategy does not take into account the detailed dependency of the lift coefficient on the slat position and mainly relies on the fact that superposition of two sinusoidal wave forms with the correct phase shift reduces the amplitude of the resultant wave form. An improved mitigation of the lift coefficients may be achieved by a tailored control strategy considering the dependency of the lift coefficient on gap size and angle of attack.

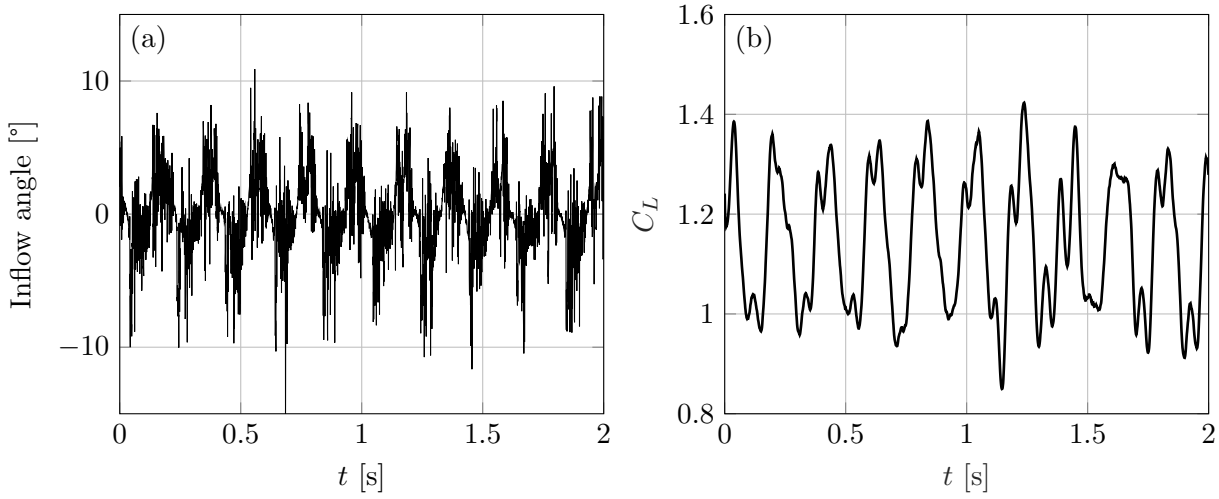

Figure 6: Inflow angle measured by X-hot-wire in the empty closed test section (a) and lift coefficient fluctuations through inflow angle fluctuations for the airfoil with a pitch angle of 10° and static slat (b).

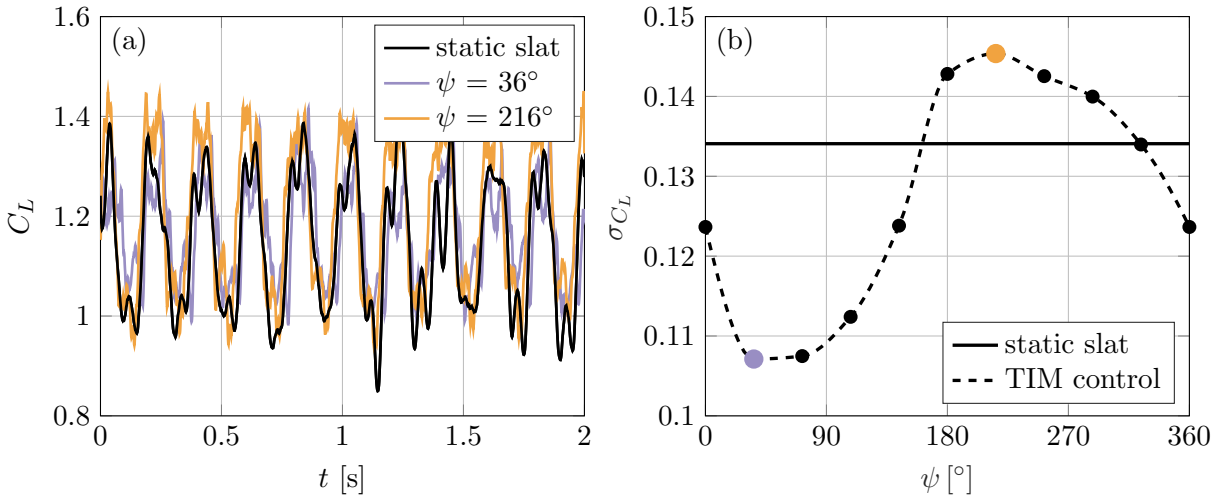

Figure 7: Lift coefficients C_L time series for static slat and TIM controlled slat with phase shifts $\psi = 36°$ and 216° (a) and standard deviation of lift coefficient σ_{C_L} of static slat and TIM controlled slat for different ψ with inflow angle fluctuations (b).

4. Conclusion

A slotted airfoil with variable gap size was tested in the wind tunnel to study the potential of mitigating load fluctuations for turbulent flow field disturbances. A detailed analysis of the aerodynamic behavior for the static slat has been performed. It is shown, that the integrated slat is increasing the maximum lift and shifting stall to much higher angles of attack from $\alpha_{max} = 10°$ to $\alpha_{max} = 30°$ compared to the clean airfoil. With variation of the static gap size different lift coefficients can be achieved. The dependence of the lift coefficient on the gap size is showing different trends for different angles of attack. So, the minimal and maximal lift do not need to be generated by the extreme gap sizes. This needs to be considered in the future control designs.

The capability to reduce lift fluctuations caused by inflow angle fluctuations was tested by dynamic variation of the slat gap size. The active slat was used to damp lift force fluctuations caused by a sinusoidal inflow angle fluctuation. To do so, the gap size was varied sinusoidally with different phase shifts relative to the inflow angle fluctuations. It was possible to reduce the standard deviation of the lift force fluctuations by 20.1 %. So, the concept of the active slat demonstrates the capability of reducing lift force fluctuations.

It is planed to investigate the aerodynamic behaviour of the airfoil with actively controlled slat, based on the results presented herein. For an advanced control of the loads the dynamic dependence of the lift coefficient on the slat gap size for every angle of attack needs to be considered. This will allow for a better fitted dynamic gap size variation and hence a probably increased mitigation of the load fluctuations. An open loop, as well as a closed loop control of the lift force will be tested. In addition, different complex turbulent inflows will be applied. This general investigation on an active slat will form a basis for validating different slat concepts. It is envisioned that the application of such a slat concept on the inner section of a full scale wind turbine will reduce load fluctuations on the blade and delay stall in the blade region which is mostly affected by it.

Acknowledgments

This work has been funded by the German Ministry of Economic Affairs and Energy (BMWi) on decision of the German Parliament in the frame of the SmartBlades2 project (funding reference no. 0324032D).

References

[1] Wächter M, Heißelmann H, Hölling M, Morales A, Milan P, Mücke T, Peinke J, Reinke N and Rinn P 2012 The turbulent nature of the atmospheric boundary layer and its impact on the wind energy conversion process *J. Turbulence* **13**:N26.
[2] Smith A M O 1975 High-lift aerodynamics *J. Aircraft* **12**(6) 501-530.
[3] Foster D N 1972 Flow around Wing Sections with High-Lift Devices *J. Aircraft* **9.3** 205-210
[4] Heißelmann H, Peinke J Hölling M 2016 Experimental airfoil characterization under tailored turbulent conditions *J. Phys: Conf. Ser.* **753** 072020
[5] Manso Jaume A and Wild J 2016 Aerodynamic design and optimization of a high-lift device for a wind turbine airfoil *New Results in Numerical and Experimental Fluid Mechanics X. Springer* 859-869
[6] Huxdorf O, Riemenschneider J, Lorsch P and Radestock M 2017 Structural design and experimental investigations of a shape-adaptive slat for wind energy rotor blades *SMART2017*
[7] Manso Jaume A, Wild J, Homeyer T, Hölling M and Peinke J 2015 Design and wind tunnel testing of a leading edge slat for a wind turbine airfoil *Proceedings of the Deutscher Windenergie Kongress (DEWEK)*